Roton-Maxon Excitation Spectrum of Bose Condensates in a Shaken Optical Lattice

Li-Chung Ha,[1] Logan W. Clark,[1] Colin V. Parker,[1] Brandon M. Anderson,[1,2] and Cheng Chin[1]
[1]James Franck Institute, Enrico Fermi Institute and Department of Physics, University of Chicago, Chicago, Illinois 60637, USA
[2]Joint Quantum Institute, University of Maryland, College Park, Maryland 20742, USA
(Received 2 August 2014; published 3 February 2015)

We present experimental evidence showing that an interacting Bose condensate in a shaken optical lattice develops a roton-maxon excitation spectrum, a feature normally associated with superfluid helium. The roton-maxon feature originates from the double-well dispersion in the shaken lattice, and can be controlled by both the atomic interaction and the lattice modulation amplitude. We determine the excitation spectrum using Bragg spectroscopy and measure the critical velocity by dragging a weak speckle potential through the condensate—both techniques are based on a digital micromirror device. Our dispersion measurements are in good agreement with a modified Bogoliubov model.

DOI: 10.1103/PhysRevLett.114.055301 PACS numbers: 67.85.-d, 03.75.Kk, 05.30.Jp, 37.10.Jk

In his seminal papers in the 1940s [1,2], L. D. Landau formulated the theory of superfluid helium-4 (He II) and showed that the energy-momentum relation (dispersion) of He II supports two types of elementary excitations: acoustic phonons and gapped rotons. This dispersion underpins our understanding of superfluidity in helium and explains many experiments on heat capacity and superfluid critical velocity. What is now called the "roton-maxon" dispersion in He II has been precisely measured in neutron scattering experiments [3,4] and is generally considered a hallmark of Bose superfluids in the strong interaction regime.

The roton-maxon dispersion carries a number of intriguing features that distinguish excitations in different regimes. The low-lying excitations are acoustic phonons with energy $E = pv_s$, where p is the momentum and v_s is the sound speed. At higher momenta, the dispersion exhibits both a local maximum at $p = p_m$ with energy $E = \Delta_m$ and a minimum at $p = p_r$ with energy $E = \Delta_r$. The elementary excitations associated with this maximum and minimum are known as maxons and rotons, respectively. The roton excitations, in particular, are known to reduce the superfluid critical velocity below the sound speed. This is best understood based on the Landau criterion for superfluidity in which the critical velocity set by the roton minimum $v_c \approx \Delta_r/p_r$ is lower than the sound speed v_s. The roton minimum also suggests the emergence of density wave order [5] and dynamical instability [6].

To explore the properties of these unconventional excitations, many theoretical works have proposed schemes for producing the roton-maxon dispersion outside of the He II system. Many proposals have been devoted to atomic systems with long-range or enhanced interactions, e.g., dipolar gases [6–8], Rydberg-excited condensates [9], or resonantly interacting gases [10]. Other candidates are 2D Bose gases [11,12], spinor condensates [13,14], and spin-orbit coupled condensates [15,16]. Experimentally, mode softening resulting from cavity-induced interaction has recently been reported [17], which provides strong evidence for an underlying rotonlike excitation spectrum.

In this Letter, we generate and characterize an asymmetric roton-maxon excitation spectrum based on a Bose-Einstein condensate (BEC) in a one dimensional (1D) shaken optical lattice. We implement Bragg spectroscopy and identify the local maximum and minimum in the dispersion associated with the maxon and roton excitations. Furthermore, by dragging a speckle potential through the BEC we show a reduction of the superfluid critical velocity in the presence of the roton dispersion.

We create the roton-maxon dispersion by loading a 3D Bose condensate into a 1D shaken (i.e., periodically phase modulated) optical lattice. The lattice shaking technique has been used previously to engineer novel band structures [18,19] and to simulate magnetism [20–22]. Here, we phase modulate the lattice to create a double-well structure in the single-particle dispersion $\epsilon_0(q)$, for which the ground state has a twofold degeneracy; see Fig. 1(a) and Ref. [21]. The double-well dispersion results from a near resonant coupling between the ground and first excited band through lattice shaking [21], and is a consequence of the parametric instability of a driven anharmonic oscillator [18]. The dispersion with quasimomentum q can be calculated based on a Floquet model [21]. A similar double-well dispersion can also be realized in a spin-orbit coupled system [23–27].

The double-well dispersion is modified by atomic interactions. Assuming the BEC is loaded into one of the two dispersion minima at quasimomentum $q = q^*$, we introduce the canonical momentum $p = q - q^*$ in the reference frame where the condensate has zero momentum and energy. The new dispersion is $\tilde{\epsilon}_0(p) = \epsilon_0(p + q^*) - \epsilon_0(q^*)$. One finds that the dispersions are no longer symmetric due to the existence of the other unoccupied

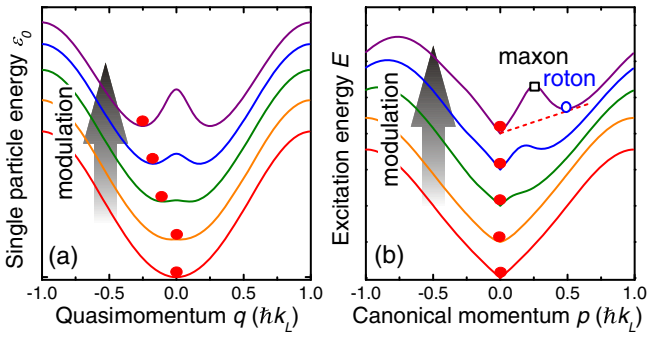

FIG. 1 (color online). Generation of roton-maxon dispersion in a shaken lattice. (a) For a single atom, the lattice modulation creates a double-well structure above a critical modulation amplitude (top three lines) [21]. In our experiment, the atoms are prepared at the minimum with zero or negative momentum ($q^* \leq 0$, red dot); see text. (b) With atomic interactions, a roton minimum (circle) and a maxon maximum (square) in the excitation spectrum can form. The dashed line indicates the critical velocity limited by the roton minimum according to the Landau criterion for superfluidity. Dispersions are upward offset with increasing modulation amplitude for clarity. The lattice reciprocal momentum is $\hbar k_L = h/\lambda$ where λ is the wavelength of the lattice beams and $h = 2\pi\hbar$ is the Planck constant.

minimum; see Fig. 1(b). Based on a modified Bogoliubov calculation (see Supplemental Material [28] and Refs. [29,30]), we diagonalize the Hamiltonian to obtain the excitation spectrum

$$E(p) = \sqrt{\bar{\epsilon}(p)^2 + 2\mu\bar{\epsilon}(p)} + \Delta\epsilon(p), \quad (1)$$

where $\bar{\epsilon}(p) = [\tilde{\epsilon}_0(p) + \tilde{\epsilon}_0(-p)]/2$, $\Delta\epsilon(p) = [\tilde{\epsilon}_0(p) - \tilde{\epsilon}_0(-p)]/2$, and μ is the chemical potential. For a system with a double-well structure in $\tilde{\epsilon}_0(p)$, the theory predicts a roton-maxon structure with the roton minimum occurring near $p = -2q^*$; see Fig. 1(b). Creation of an "artificial roton" in the dispersion minimum of an analogous spin-orbit coupled system was theoretically proposed in Ref. [15].

Our experiment to detect this unusual dispersion starts with an almost pure cesium condensate of $N_0 = 30\,000$ atoms loaded into a crossed beam optical dipole trap (wavelength $\lambda = 1064$ nm) with trap frequencies $(\omega_x, \omega_y, \omega_z) = 2\pi \times (9.3, 27, 104)$ Hz [21]. We turn on an additional 1D optical lattice by retroreflecting one of the dipole trap beams in the $x - y$ plane at 40° with respect to the x axis. The lattice depth is approximately $V = 7\ E_R$, where $E_R = h \times 1.325$ kHz is the photon recoil energy of the lattice beam. The lattice potential is phase modulated at 7.3 kHz which is 0.7 kHz blue detuned from the ground to first excited band transition at $q = 0$. The phase modulation creates admixed bands, and the ground band develops two minima in its dispersion [21]. We preferentially load the BEC into one of the minima by providing a momentum kick before phase modulating the lattice [21]. We define the

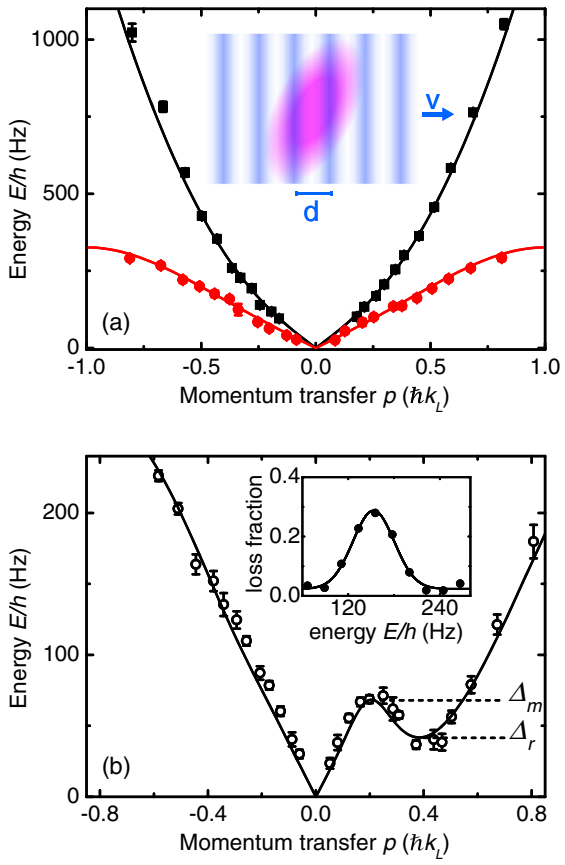

FIG. 2 (color online). Excitation spectra. (a) We measure the excitation spectra with $N_0 = 30\,000$ atoms in a harmonic trap (square) and in a stationary lattice (circle) with DMD-based Bragg spectroscopy. The inset illustrates the moving optical potential with velocity v and periodicity d created by the DMD on the BEC (tilted ellipse); see text. The solid lines correspond to the Bogoliubov model with chemical potentials equal to the trap-averaged values. (b) For a BEC with $N_0 = 9000$ atoms loaded in a shaken optical lattice, we measure the excitation spectrum along the lattice direction. The modulation amplitude (peak to peak) is $\Delta x = 33$ nm. The solid line is the best fit based on Eq. (1). The inset shows a typical atom loss spectrum taken at $k = -0.38\ k_L$. In both panels, the scattering length is $a = 47\ a_0$.

direction of the kick as negative, and thus, the BEC has a negative momentum $q = q^* < 0$ and the roton minimum is expected at $p = 2|q^*|$; see Fig. 1(b).

To probe the dispersion we perform Bragg spectroscopy [31] by illuminating the atoms with a sinusoidal potential moving along the direction of the shaken lattice. The potential is created from a programmable digital micromirror device (DMD) and a 789 nm laser, which provides a repulsive dipole force. The DMD potential with velocity v and periodicity d [see Fig. 2(a) inset] induces a Raman coupling between the condensate with $p = 0$ and finite momentum states with $p = h/d$. When the Raman detuning $E = pv$ matches the energy of the finite momentum state $E(p)$, a resonant transfer will remove atoms from the condensate. We illuminate the atoms with the moving

potential for 40 ms and measure the residual condensate particle number after a 30 ms time of flight (TOF). The dispersion can be mapped out by finding the energy which gives the strongest reduction of atom number in the condensate for each momentum p.

To test this technique, we compare the dispersions of the BEC in a harmonic trap and that in a $V = 7\ E_R$ unshaken lattice to Bogoliubov calculations; see Fig. 2(a). The measurement agrees well with the Bogoliubov spectrum using the measured trap-averaged chemical potentials $\mu = h \times 120$ Hz without the lattice and $\mu = h \times 150$ Hz with the lattice.

We now consider the dispersion of a BEC in a shaken optical lattice, where the roton feature is expected. Here, we observe a distinct difference between the excitations at positive vs negative momentum. We work with a modulation amplitude (peak to peak) of $\Delta x = 33$ nm which guarantees a strong double-well feature. Figure 2(b) shows the dispersion measurement, which contains a clear roton-maxon feature at positive momentum (hereafter, the roton direction). In contrast, we do not see this feature for negative momentum (hereafter, the nonroton direction).

We compare the measured roton spectrum with the model in Eq. (1). Constraining the model to the experimental parameters only yields qualitative agreement likely due to interaction effects [32] which effectively modify the modulation amplitude Δx and lattice depth V. Thus, we fit the data with Eq. (1) and find the best fit to have $\mu = h \times 58(4)$ Hz, $V = 5.9(1)\ E_R$, and $\Delta x = 49(3)$ nm. The low chemical potential is expected and comes from the lower condensate number as well as the weaker, momentum dependent atomic interactions in the admixed band.

The roton energy is determined by atomic interactions and can be controlled by tuning the scattering length. To demonstrate this, we prepare samples with the usual procedure but at a higher scattering length $a = 70\ a_0$ followed by ramping the magnetic field to reach the desired scattering length [33]. We measure the excitation spectrum in the roton direction with $p > 0$ at six different scattering lengths, shown in Fig. 3(a).

We adopt a global fit to the data in Fig. 3(a) based on Eq. (1) to determine the roton energy Δ_r and the maxon energy Δ_m. Our observation shows that we can experimentally tune the scattering length to vary the roton energy by a factor of 3. Furthermore, we can use scaling arguments to distinguish the behavior of rotons and maxons from the more conventional phonons. For small chemical potentials, the excitation energy for phonons is well known to scale as $\mu^{1/2}$, while the roton and maxon energies are expected to depend linearly on μ; see Supplemental Material [28]. Furthermore, for an adiabatic ramp of the scattering length, the chemical potential should scale as $\mu = n_0 g \propto a^{2/5}$ where $g \propto a$ is the interaction strength, and the condensate density in the harmonic trap is $n_0 \propto a^{-3/5}$ [34]. Therefore, we plot the extracted roton and maxon energies as a function of $a^{2/5}$ as a proxy for the chemical potential; see Fig. 3(b). The observed linear dependence confirms the expected scaling for rotons and maxons.

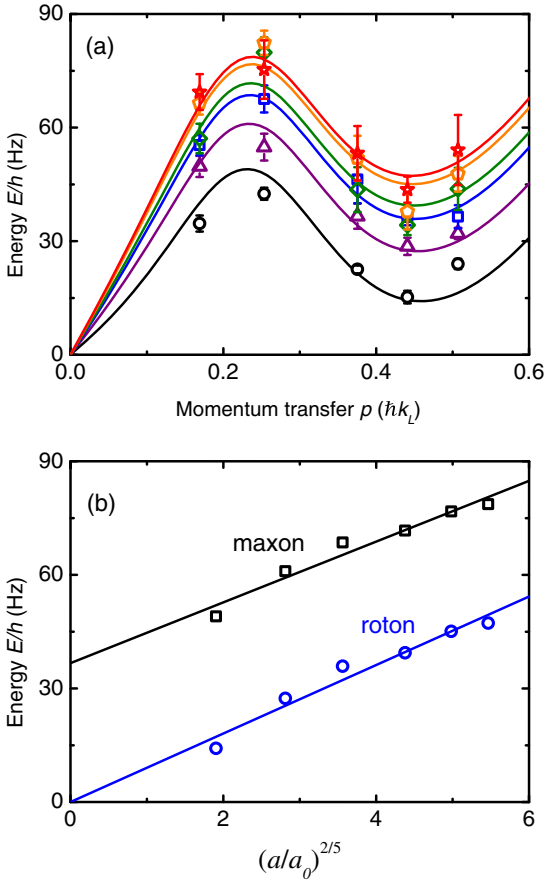

FIG. 3 (color online). Roton or maxon energy vs scattering length. (a) We measure the excitation spectra at different scattering lengths $a/a_0 = 5$ (circle), 13 (triangle), 24 (square), 40 (diamond), 55 (pentagon), and 70 (star). The condensate number is $N_0 = 9000$. Solid curves are fits based on Eq. (1). A global optimization procedure gives $V = 6.7(2)\ E_R$ and $\Delta x = 43(3)$ nm. (b) Roton energies (circle) and maxon energies (square) extracted from the fits in panel (a) are shown at different scattering lengths. Solid curves are fits based on $\Delta_r = A(a/a_0)^{2/5}$ and $\Delta_m = B + C(a/a_0)^{2/5}$, from which we obtain $A = h \times 9(1)$ Hz, $B = h \times 37(9)$ Hz, and $C = h \times 8(1)$ Hz.

One significant consequence of the roton dispersion is the suppressed superfluid critical velocity v_c. We measure the critical velocity of the BEC loaded into the shaken lattice by projecting a moving speckle pattern using the DMD. Instead of using a single laser beam [35–37] or a lattice with a definite spatial frequency [38], our speckle pattern contains a broad spectrum of wave numbers up to the resolution ($k \approx 0.55\ k_L$) of our projection system. Furthermore, the potential remains locally perturbative ($\approx h \times 1.1$ Hz) to prevent vortex proliferation [39–41]. When the velocity of the speckle pattern reaches or exceeds the critical velocity, atoms are excited from the condensate. To prevent excitation in the low density tail [38], we

digitally mask out the region of the speckle pattern which could overlap with the edge of the cloud.

We observe a clear threshold in speckle velocity above which the condensate number decreases; see Fig. 4(a). The experimental sequence is similar to that used for Bragg spectroscopy: we illuminate the cloud with a moving speckle pattern for 100 ms followed by a 30 ms TOF. To find the critical velocity, we fit the remaining condensate number with a constant value intersecting a linear decay. The intersection point determines the critical velocity v_c. Above a critical value, we observe that the condensate fraction decreases linearly with the speckle velocity. This is consistent with a previous observation of the critical velocity in a Bose superfluid [38], along with a recent calculation [42].

In order to understand the emergence of the roton-maxon dispersion, we measure critical velocity in both the roton direction $p > 0$ and the nonroton direction $p < 0$ with increasing modulation amplitude Δx; see Fig. 4(b). In order to maintain a comparable chemical potential, we prepare the samples with a large $\Delta x = 33$ nm and slowly ramp Δx to the desired value. For small final $\Delta x < 12$ nm, v_c is the same in both directions and decreases as we approach the critical value $\Delta x_c \approx 12$ nm (phonon mode softening). When the gas enters the ferromagnetic phase ($\Delta x > 12$ nm) [21], v_c increases immediately along the nonroton direction, while in the roton direction v_c remains small.

We compare the measurement with the critical velocity based on the Landau criterion $v_L = \min|E(p)/p|$. As the experiment conditions closely resemble those in Fig. 2(b), we evaluate the critical velocity with $\mu = h \times 58$ Hz, $V = 5.9\ E_R$, and Δx scaled by 1.5, the parameters which best fit that dispersion measurement. The calculated v_L, shown as dashed lines in Fig. 4(b), displays a disparity between the roton and nonroton directions for $\Delta x > 15$ nm, in agreement with our observation. Our critical velocities, however, are significantly lower than v_L. In early BEC experiments [36,37], low critical velocities were observed and explained by the large obstacles that disrupt the superflow and spin off vortices [39–41]. In our experiment with weak speckle potential, a likely scenario is that the critical velocity is limited by excitations generated in the low density regions above and below the cloud along the DMD projection axis.

In conclusion, we observe a roton-maxon dispersion of a BEC in a shaken 1D optical lattice based on three pieces of evidence: the many-body excitation spectrum, the dependence of the excitation energies on the atomic interactions, and the superfluid critical velocity measurement. Our results agree well with the Bogoliubov calculation and suggest that the roton or maxon excitations are distinct from acoustic phonons. Our experiment demonstrates that shaken optical lattices are a convenient platform to generate new types of quasiparticles in a dilute atomic gas, allowing future study of their dynamics, stability, and interactions.

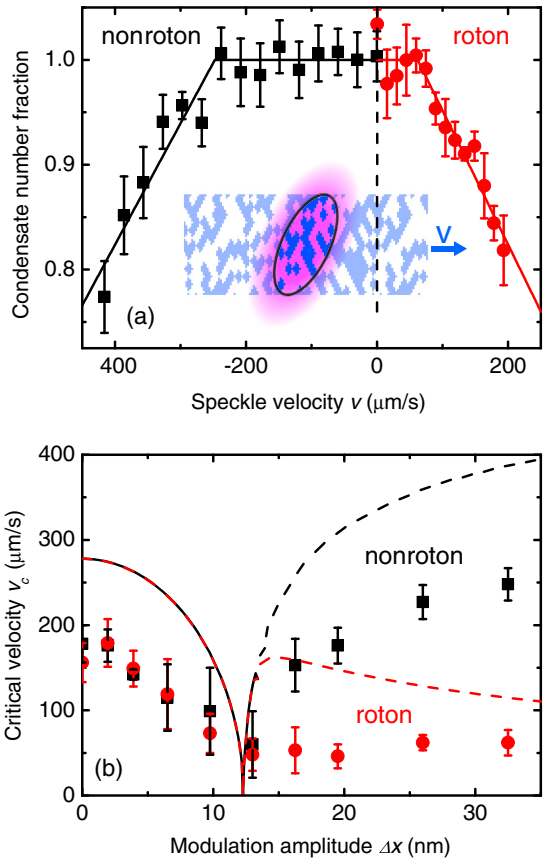

FIG. 4 (color online). Superfluid critical velocity. (a) We measure the residual condensate number fraction after dragging a speckle pattern through the center of the cloud at different velocities v along the roton direction ($p > 0$, solid dots) and the nonroton direction ($p < 0$, solid squares). The solid lines are fits used to determine the critical velocity. The inset illustrates the experimental scheme; see text. (b) Critical velocities as a function of modulation amplitude are shown. Above the critical modulation amplitude, $\Delta x > 12$ nm, the critical velocity is significantly lower in the roton direction. Our measurement is compared with the critical velocity calculated from Eq. (1) using the Landau criterion (dashed lines). In both panels, the scattering length is $a = 47\ a_0$ and the initial condensate number is $N_0 = 9000$.

For instance, knowing the quasiparticle dispersion should allow a future experiment to create macroscopic numbers of rotons, leading to possible roton condensation [42,43], and separation of the rotons into domains. *In situ* imaging would allow direct observation of the temporal evolution of such states.

We thank K. Jiménez García for discussion and careful reading of the article, and U. Eismann and E. Hazlett for assistance in the early phase of the experiment. L.-C. H. is supported by the Grainger Fellowship and the Taiwan Government Scholarship. L. W. C. is supported by the NDSEG Fellowship. This work was supported by NSF MRSEC Grant No. DMR-1420709, NSF Grant No. PHY-0747907 and ARO-MURI Grant No. W911NF-14-1-0003.

[1] L. D. Landau, J. Phys. (Moscow) **5**, 71 (1941).
[2] L. D. Landau, J. Phys. (Moscow) **11**, 91 (1947).
[3] D. G. Henshaw and A. D. B. Woods, Phys. Rev. **121**, 1266 (1961).
[4] H. R. Glyde, *Excitations in Liquid and Solid Helium* (Clarendon, Oxford, 1994).
[5] T. Schneider and C. P. Enz, Phys. Rev. Lett. **27**, 1186 (1971).
[6] L. Santos, G. V. Shlyapnikov, and M. Lewenstein, Phys. Rev. Lett. **90**, 250403 (2003).
[7] R. M. Wilson, S. Ronen, J. L. Bohn, and H. Pu, Phys. Rev. Lett. **100**, 245302 (2008).
[8] D. H. J. O'Dell, S. Giovanazzi, and G. Kurizki, Phys. Rev. Lett. **90**, 110402 (2003).
[9] N. Henkel, R. Nath, and T. Pohl, Phys. Rev. Lett. **104**, 195302 (2010).
[10] Y. Yunomae, D. Yamamoto, I. Danshita, N. Yokoshi, and S. Tsuchiya, Phys. Rev. A **80**, 063627 (2009); S. C. Cormack, D. Schumayer, and D. A. W. Hutchinson, Phys. Rev. Lett. **107**, 140401 (2011); R. Rota, F. Tramonto, D. E. Galli, and S. Giorgini, Phys. Rev. B **88**, 214505 (2013).
[11] U. R. Fischer, Phys. Rev. A **73**, 031602(R) (2006).
[12] F. S. Nogueira and H. Kleinert, Phys. Rev. B **73**, 104515 (2006).
[13] R. W. Cherng and E. Demler, Phys. Rev. Lett. **103**, 185301 (2009).
[14] M. Matuszewski, Phys. Rev. Lett. **105**, 020405 (2010).
[15] J. Higbie and D. M. Stamper-Kurn, Phys. Rev. Lett. **88**, 090401 (2002).
[16] W. Zheng and Z. Li, Phys. Rev. A **85**, 053607 (2012); G. I. Martone, Y. Li, L. P. Pitaevskii, and S. Stringari, Phys. Rev. A **86**, 063621 (2012); W. Zheng, Z.-Q. Yu, X. Cui, and H. Zhai, J. Phys. B **46**, 134007 (2013).
[17] R. Mottl, F. Brennecke, K. Baumann, R. Landig, T. Donner, and T. Esslinger, Science **336**, 1570 (2012).
[18] N. Gemelke, E. Sarajlic, Y. Bidel, S. Hong, and S. Chu, Phys. Rev. Lett. **95**, 170404 (2005).
[19] H. Lignier, C. Sias, D. Ciampini, Y. Singh, A. Zenesini, O. Morsch, and E. Arimondo, Phys. Rev. Lett. **99**, 220403 (2007).
[20] J. Struck, C. Ölschläger, R. Le Targat, P. Soltan-Panahi, A. Eckardt, M. Lewenstein, P. Windpassinger, and K. Sengstock, Science **333**, 996 (2011).
[21] C. V. Parker, L.-C. Ha, and C. Chin, Nat. Phys. **9**, 769 (2013).
[22] G. Jotzu, M. Messer, R. Desbuquois, M. Lebrat, T. Uehlinger, D. Greif, and T. Esslinger, Nature (London) **515**, 237 (2014).
[23] Y.-J. Lin, K. Jiménez-García, and I. B. Spielman, Nature (London) **471**, 83 (2011).
[24] L. W. Cheuk, A. T. Sommer, Z. Hadzibabic, T. Yefsah, W. S. Bakr, and M. W. Zwierlein, Phys. Rev. Lett. **109**, 095302 (2012).
[25] C. Hamner, C. Qu, Y. Zhang, J. Chang, M. Gong, C. Zhang, and P. Engels, Nat. Commun. **5**, 4023 (2014).
[26] S.-C. Ji, J.-Y. Zhang, L. Zhang, Z.-D. Du, W. Zheng, Y.-J. Deng, H. Zhai, S. Chen, and J.-W. Pan, Nat. Phys. **10**, 314 (2014).
[27] Z. Fu, L. Huang, Z. Meng, P. Wang, L. Zhang, S. Zhang, H. Zhai, P. Zhang, and J. Zhang, Nat. Phys. **10**, 110 (2014).
[28] See Supplemental Material at http://link.aps.org/supplemental/10.1103/PhysRevLett.114.055301 for experimental details and a theoretical model.
[29] A. Eckardt, P. Hauke, P. Soltan-Panahi, C. Becker, K. Sengstock, and M. Lewenstein, Europhys. Lett. **89**, 10010 (2010).
[30] J. Struck *et al.*, Nat. Phys. **9**, 738 (2013).
[31] R. Ozeri, N. Katz, J. Steinhauer, and N. Davidson, Rev. Mod. Phys. **77**, 187 (2005).
[32] W. Zheng, B. Liu, J. Miao, C. Chin, and H. Zhai, Phys. Rev. Lett. **113**, 155303 (2014).
[33] C. Chin, R. Grimm, P. Julienne, and E. Tiesinga, Rev. Mod. Phys. **82**, 1225 (2010).
[34] C. J. Pethick and H. Smith, *Bose-Einstein Condensation in Dilute Gases*, 2nd ed. (Cambridge University Press, Cambridge, England, 2008).
[35] R. Desbuquois, L. Chomaz, T. Yefsah, J. Léonard, J. Beugnon, C. Weitenberg, and J. Dalibard, Nat. Phys. **8**, 645 (2012).
[36] C. Raman, M. Köhl, R. Onofrio, D. S. Durfee, C. E. Kuklewicz, Z. Hadzibabic, and W. Ketterle, Phys. Rev. Lett. **83**, 2502 (1999).
[37] R. Onofrio, C. Raman, J. M. Vogels, J. R. Abo-Shaeer, A. P. Chikkatur, and W. Ketterle, Phys. Rev. Lett. **85**, 2228 (2000).
[38] D. E. Miller, J. K. Chin, C. A. Stan, Y. Liu, W. Setiawan, C. Sanner, and W. Ketterle, Phys. Rev. Lett. **99**, 070402 (2007).
[39] T. Winiecki, B. Jackson, J. F. McCann, and C. S. Adams, J. Phys. B **33**, 4069 (2000).
[40] T. Frisch, Y. Pomeau, and S. Rica, Phys. Rev. Lett. **69**, 1644 (1992).
[41] J. S. Stießberger and W. Zwerger, Phys. Rev. A **62**, 061601 (R) (2000).
[42] G. Baym and C. J. Pethick, Phys. Rev. A **86**, 023602 (2012).
[43] L. P. Pitaevskii, Zh. Eksp. Teor. Fiz. **39**, 423 (1984) [JETP Lett. **39**, 511 (1984)].